IJID Regions 6 (2023) 29–41

Contents lists available at ScienceDirect

IJID Regions

journal homepage: www.elsevier.com/locate/ijregi

# Effects of hydrometeorological and other factors on SARS-CoV-2 reproduction number in three contiguous countries of tropical Andean South America: a spatiotemporally disaggregated time series analysis

Josh M. Colston[a,§], Patrick Hinson[b,§], Nhat-Lan H. Nguyen[b,§], Yen Ting Chen[c,§], Hamada S. Badr[d], Gaige H. Kerr[e], Lauren M. Gardner[f], David N. Martin[g], Antonio M. Quispe[h], Francesca Schiaffino[i,j], Margaret N. Kosek[j,*], Benjamin F. Zaitchik[e]

[a] Division of Infectious Diseases and International Health, University of Virginia School of Medicine, Charlottesville, VA, 22903, USA
[b] College of Arts and Sciences, University of Virginia, VA, USA
[c] Department of Emergency Medicine, Chi-Mei Medical Center, Tainan, Taiwan
[d] Department of Earth and Planetary Sciences, Johns Hopkins Krieger School of Arts and Sciences, Baltimore, MD, 21218, USA
[e] Department of Environmental and Occupational Health, Milken Institute School of Public Health, George Washington University, Washington, DC, USA
[f] Department of Civil and Systems Engineering, Johns Hopkins University, Baltimore, MD, USA
[g] Claude Moore Health Sciences Library, University of Virginia School of Medicine, VA, USA
[h] Postgraduate School, Universidad Continental, Lima, Peru
[i] Faculty of Veterinary Medicine, Universidad Peruana Cayetano Heredia, Lima, Peru;
[j] Division of Infectious Diseases and International Health and Public Health Sciences, University of Virginia School of Medicine, Charlottesville, VA, 22903, USA

ARTICLE INFO

*Keywords:*
coronavirus
COVID-19
SARS-CoV-2
climate
hydrometeorology
pandemic disease
Latin America
Peru
Ecuador
Colombia

ABSTRACT

*Background:* The COVID-19 pandemic has caused societal disruption globally, and South America has been hit harder than other lower-income regions. This study modeled the effects of six weather variables on district-level SARS-CoV-2 reproduction numbers ($R_t$) in three contiguous countries of tropical Andean South America (Colombia, Ecuador, and Peru), adjusting for environmental, policy, healthcare infrastructural and other factors.
*Methods:* Daily time-series data on SARS-CoV-2 infections were sourced from the health authorities of the three countries at the smallest available administrative level. $R_t$ values were calculated and merged by date and unit ID with variables from a unified COVID-19 dataset and other publicly available sources for May–December, 2020. Generalized additive models were fitted.
*Findings:* Relative humidity and solar radiation were inversely associated with SARS-CoV-2 $R_t$. Days with radiation above 1000 kJ/m$^2$ saw a 1.3% reduction in $R_t$, and those with humidity above 50% recorded a 0.9% reduction in $R_t$. Transmission was highest in densely populated districts, and lowest in districts with poor healthcare access and on days with lowest population mobility. Wind speed, temperature, region, aggregate government policy response, and population age structure had little impact. The fully adjusted model explained 4.3% of $R_t$ variance.
*Interpretation:* Dry atmospheric conditions of low humidity increase district-level SARS-CoV-2 reproduction numbers, while higher levels of solar radiation decrease district-level SARS-CoV-2 reproduction numbers — effects that are comparable in magnitude to population factors like lockdown compliance. Weather monitoring could be incorporated into disease surveillance and early warning systems in conjunction with more established risk indicators and surveillance measures.
*Funding:* NASA's Group on Earth Observations Work Programme (16-GEO16-0047)

## Introduction

Since its discovery in Wuhan, China in December 2019, the SARS-CoV-2 virus has swept the globe, overwhelming national healthcare services with successive waves and variants, and causing widespread socioeconomic insecurity and societal unrest in virtually every country of the world (Onyeaka et al., 2021; Wang et al., 2020). At the time of writing, over 533 million infections and 6.3 million deaths globally had

* Corresponding author: Margaret N. Kosek, Division of Infectious Diseases and International Health and Public Health Sciences, University of Virginia School of Medicine, Charlottesville, VA, 22903, USA.
*E-mail address:* mkosek@virginia.edu (M.N. Kosek).
§ These authors contributed equally.

https://doi.org/10.1016/j.ijregi.2022.11.007
Received 19 July 2022; Received in revised form 14 November 2022; Accepted 15 November 2022

been attributed to the virus (Center for Systems Science and Engineering (CSSE) at Johns Hopkins University (JHU), 2021). However, the true toll is undoubtedly far higher than official statistics, and may have surpassed 3.8 billion infections (40% of the global population) and 15 million deaths (Barber et al., 2022).

South America has been hit harder by the coronavirus disease (COVID-19) pandemic than other predominantly lower-income regions, with some of the highest excess mortality and case fatality rates (CFR). Its 58 million confirmed cases (> 256 million estimated total) have led to over 1.3 million confirmed deaths (> 1.7 million total), putting further strain on a region where many countries struggle with political instability, humanitarian crises, and income inequality (Barber et al., 2022; Center for Systems Science and Engineering (CSSE) at Johns Hopkins University (JHU), 2021; The Lancet, 2020; Wang et al., 2022).

From the early days of the pandemic, questions were raised about the possible influences of climate and meteorology on the transmission of the virus, given the known sensitivity of other respiratory viruses to these factors (Audi et al., 2020; O'Reilly et al., 2020). One early study noted that COVID-19 community transmission at the beginning of the pandemic was especially high along a temperate, mid-latitude belt of the northern hemisphere (Sajadi et al., 2020). However, it was already clear by that early stage that the influence of such factors was small relative to that of population density and age structure, and timing of, and compliance with, non-pharmaceutical interventions (NPIs), such as lockdowns, travel restrictions, and hygiene measures. Initial research rightly prioritized these more proximal drivers (Carlson et al., 2020; Meyer et al., 2020; Zaitchik et al., 2020).

With the pandemic in its third year, and with the likely prospect that SARS-CoV-2 will continue to circulate as an endemic, seasonal, and vaccine-preventable virus for the foreseeable future (Telenti et al., 2021), attention has turned again to the role of meteorological factors in COVID-19 transmission (Audi et al., 2020; Chen et al., 2021). The demand for real-time data with which to track the global health crisis has prompted a proliferation of online repositories and interfaces, which curate and disseminate epidemiological data with a global scope and increasing spatial and temporal resolutions (Badr et al., 2021; Dong et al., 2020; Wang et al., 2022).

For further analysis, disease data can be matched by date and location to high-resolution estimates of spatiotemporal variation in environmental and hydrological conditions derived from remote sensing and climate models (Colston et al., 2018). Numerous studies have applied this approach to subnational unit-level case reports in an attempt to model associations between hydrometeorological variables and SARS-CoV-2 outcomes (Ma et al., 2021; Sera et al., 2021). However, there is considerable variation in how confounding factors and errors in case reporting are captured (Mecenas et al., 2020; Quintana et al., 2021), and a disproportionate emphasis on high-income countries, mostly in the temperate mid-latitudes (Kerr et al., 2021).

The aim of this study was to model the effects of weather on the district-level SARS-CoV-2 reproduction number ($R_t$) for three contiguous countries of tropical Andean South America (Colombia, Ecuador, and Peru), with an expanded suite of hydrometeorological parameters and after further adjusting for environmental, policy, healthcare infrastructural, and other factors during the first wave of the epidemic, when a single circulating variant predominated and there was no population-level immunity that contributed to transmission dynamics.

## Methods

### *Scope of analysis*

The three tropical Andean South American countries of Colombia, Ecuador, and Peru were chosen for this analysis, since together they constitute a large contiguous territory, with a roughly even split between the northern and southern hemispheres, and broadly divisible into coastal, highland, and interior regions. Furthermore, all three countries have comparable health information system capacity and make publicly available daily reports of new COVID-19 cases at high geographical resolution. The analysis was restricted to the mainland areas of the three countries, excluding outlying island territories, and to the period from May to December, 2020, during which transmission of the virus was fully established and NPIs were in place (Sera et al., 2021), but before the emergence of major variants of concern and the introduction of vaccines.

### *Epidemiological data*

Daily time series data on confirmed SARS-CoV-2 infections were sourced from national health authority websites at the smallest available administrative level (Colombian municipalities, Ecuadorian cantons, and Peruvian districts, hereafter generically referred to as 'districts') (Robalino et al., 2021; Instituto Nacional de Salud Colombiano, 2021; Ministerio de Salud Peruano, 2021). These data were used to calculate district-level daily $R_t$ using EpiNow2, an R package for estimating time-varying epidemiological parameters of SARS-CoV-2 from subnational case notification data, accounting for right truncation, underreporting, and uncertain reporting delays and incubation periods (Abbott et al., 2020).

Daily, district-level $R_t$ estimates were treated as the outcome variable for the analysis. These are interpreted as the mean number of new infections caused by a single infected person on a given day in a given district. If a district records zero cases for an extended period, its daily $R_t$ will converge on a default value of 1, which is difficult to interpret in the absence of actual disease. However, because the calculation of $R_t$ accounts for the disease incubation period, the metric lags the cases used to calculate it, so changes in $R_t$ may precede increases and decreases in case counts by several weeks. It is therefore possible for a district to have a daily $R_t$ of greater than 1 while reporting zero cases, due to the delay in increases in transmission being reflected in case reporting.

Due to the high resolution and inclusion of many remote and sparsely populated districts in the dataset, there was a large proportion of unit-days with zero reported cases of COVID-19 (75.5%). Therefore, all unit-days in which both a) no cases were reported and b) $R_t$ had a calculated value of between 0.95 and 1.05 were excluded. The purpose of this was to restrict the analysis to observations with interpretable outcome values relevant to the research question, and to increase the variability and achieve a more Gaussian distribution of the outcome.

### *Hydrometeorological data*

Hydrometeorological data were sourced from the unified COVID-19 dataset compiled by Badr and colleagues (Badr et al., 2021), in which variables were in turn extracted from the second-generation North American Land Data Assimilation System (NLDAS-2) and the fifth-generation European Centre for Medium-Range Weather Forecasts (ECMWF) atmospheric reanalysis of the global climate (ERA5) at administrative unit centroids (Center for International Earth Science Information Network (CIESIN), 2016; Hersbach et al., 2020; Xia et al., 2012). Both datasets perform well in validation studies (Tarek et al., 2020; Xia et al., 2012) and are comparable to those used in retrospective infectious disease modeling (Colston et al., 2019), with the advantage that their much shorter latency periods (4–6 days) make them better suited for prospective forecasting of disease dynamics (Badr et al., 2021). All available hourly, population-weighted ERA5 and NLDAS values since January 1, 2020 were extracted, aggregated to daily mean or total values, and matched by date and district to the $R_t$ values.

The following variables were included as the main exposures of interest, based on their documented or hypothesized associations with SARS-CoV-2: near surface air temperature (°C) (Morris et al., 2021; Rubin et al., 2020); relative humidity (%) (Ahlawat et al., 2020); solar radiation (kJ/m$^2$) (Ma et al., 2020); total precipitation volume (mm) (Shenoy et al., 2022); average 10 m above ground wind

**Table 1**
Definitions of variables used in the analysis

| Variable | Units/categories | Temporal resolution | Spatial resolution | Source |
|---|---|---|---|---|
| **COVID-19 diagnoses** | Positive cases | Daily total | Colombia: 2nd administrative level (municipalities)<br>Ecuador: 2nd administrative level (cantons)<br>Peru: 3rd administrative level (districts) | (Instituto Nacional de Salud Colombiano, 2021)<br>(Robalino et al., 2021)<br>(Ministerio de Salud Peruano, 2021) |
| **Effective reproduction number ($R_t$)** | Secondary cases per index case | Daily | District | EpiNow2 (Abbott et al., 2020) |
| **Government policy response stringency** | % | Daily | National | OxCGRT (Hale et al., 2021) |
| **Healthcare accessibility** | Minutes of travel time to nearest health facility by motor transport | Static (2020) | District-level average | Malaria Atlas Project (Weiss et al., 2020) |
| **Natural region** | Coastal, highland, interior | Static | District | (INEI/Perú, 2013; Instituto Geografico Agustin Codazzi, 2014; This is Ecuador, 2021) |
| **Population age structure** | % population ≥ 65 years of age | Static (2020) | District-level average | WorldPop (Tatem, 2017) |
| **Population density** | Population/km$^2$ | | | |
| **Population mobility: residential** | % change relative to baseline | Daily | Province | Google (Google LLC, 2022) |
| **Air temperature** | ˚C | Daily average | District-level average | ERA5 (Hersbach et al., 2020, p. 5) |
| **Precipitation** | mm | | | |
| **Specific humidity** | g/kg | | | |
| **Soil moisture** | m$^3$/m$^3$ | | | |
| **Solar radiation** | kJ/m$^2$ | | | |
| **Wind speed** | m/s | | | |

speed (m/s) (Majumder and Ray, 2021). In addition, average volumetric soil moisture (m$^3$/m$^3$) was included as a negative control exposure (Sanderson et al., 2018), since it is a variable presumed to affect infectious disease transmission through its influence on pathogen survival on surfaces and fomites (Colston et al., 2019), which is thought to be at most only a secondary mode of SARS-CoV-2 transmission (Karia et al., 2020). Specific humidity (kg/kg) estimates were excluded from the main analysis due to their being highly correlated with temperature in this dataset ($\rho$ = 0.88), and only included in a secondary analysis reported in the **supplementary appendix**.

*Covariate data*

The following variables (summarized in Table 1) were included as covariates to adjust for their potential confounding effects on the main associations of interest:

**Natural regions:** To account for potential residual confounding factors due to geographical and topographical differences across the three countries that may affect disease transmission (Fernandes et al., 2021), their territories were grouped into three broad, cross-cutting ecological zones, based on the 'natural region' categories used by the Peruvian national statistical authority — coastal, highland (the Andes), and interior (the Amazon and Orinoco basins) (INEI/Perú, 2013; Instituto Geografico Agustin Codazzi, 2014; This is Ecuador, 2021). These were deemed to be less arbitrary from the point of view of transmission and meteorological dynamics than alternative groupings based on political divisions, such as higher-level administrative units. The three regions are shown in Fig. 3d.

**Population density:** Densely populated urban areas are often struck earlier and harder by epidemics due to their roles as transport hubs and the increased contact rates between susceptible and infectious individuals (Smith et al., 2021). Since sparsely populated areas may also differ systematically in the climatic conditions that they experience, population density was included as a potentially confounding covariate in this analysis and calculated as the district-level zonal mean value extracted from the WorldPop raster of global population distribution (Tatem, 2017).

**Population age structure:** Since the symptomaticity and severity of SARS-CoV-2 infection increase with age (Mueller et al., 2020), areas with a larger proportion of their population in the more susceptible elderly age groups may have higher rates of case reporting and infectiousness. Population age structure varies geographically to a considerable degree; therefore, the proportion of a district's population that was over the age of 65 years was calculated from the WorldPop raster of population per 5-year age group and included in the model.

**Access to healthcare facilities:** The time it takes to travel to a health facility to seek care also varies geographically as a function of population density, transport infrastructure, and local topography (Weiss et al., 2020). Connectivity has been shown to influence variation in SARS-CoV-2 outbreaks in sub-Saharan Africa (Rice et al., 2021), while travel time to seek care might affect contact rates between infected and susceptible individuals or the probability that infected persons are treated and registered in health information systems. The district-level mean travel times to the nearest healthcare facility using motorized transport in 2020 were extracted using zonal statistics from the geographical estimates published by Weiss and colleagues (Weiss et al., 2020).

**Government policy response data:** The timing and stringency with which national governments introduced public health interventions such as travel restrictions, school closures, and bans on gatherings and public events are major factors influencing geographical variation in the trajectory of the pandemic (Haug et al., 2020; Sera et al., 2021; Smith et al., 2021). The Oxford Covid-19 Government Response Tracker (OxCGRT) project collates information on numerous government policy responses into a publicly available database, assigns them scores reflecting their strictness, and aggregates these into policy metrics including a stringency index (Hale et al., 2021). This was included as a national-level, time-varying covariate in this analysis.

**Population mobility:** Compliance with NPI mandates and recommendations differs among subnational populations, leading to variation in transmission risk (Morales-Vives et al., 2022; Uddin et al., 2021). As a proxy indicator for compliance with social distancing, lockdown measures, and travel restrictions, population mobility metrics were sourced from Google's Community Mobility Reports (Google LLC, 2022) These indicators track trends in Android smartphone users' movements over time, relative to a pre-pandemic baseline, by subnational region and for six categories of location (Google LLC, 2022). The 'residential' metric was used and merged with the database by date at the first adminis-

trative unit level (hereafter generically referred to as 'provinces'), since coverage was more complete at this level than for districts. This variable can be interpreted as the percent change in time spent in residential areas compared with before the pandemic, with a higher value therefore corresponding to greater population compliance with social distancing or lockdowns. The Google mobility dataset includes intentional gaps for unit dates that do not meet a quality and privacy threshold, and which are to be considered 'true unknowns'; therefore, these intermittent missing values were substituted using linear interpolation by date within each province (Google LLC, 2022).

*Statistical analysis:*

Variables were merged based on district/province ID and date, and highly skewed variables were normalized using ordered quantile (ORQ) transformation. A generalized additive model (GAM) was fitted to the $R_t$ outcome, assuming a Gaussian distribution, log link, and REML smoothing parameter estimation method. Cubic spline terms with three degrees of freedom were specified for all continuous exposure variables to account for non-linearity. Natural regions were modeled as a factor variable with the coastal region as the reference category. The model therefore has the form:

$$R_{t,d} \sim gaussian(\mu_{t,d}) \quad (1)$$

$$\begin{aligned}\log(\mu_{t,d}) = {} & f_1(temperature_{t,d}) + f_2(ORQ(precipitation)_{t,d}) \\ & + f_3(moisture_{t,d}) + f_4(radiation_{t,d}) + f_5(humidity_{t,d}) \\ & + f_6(ORQ(wind)_{t,d}) + f_7(ORQ(accessibility)_d) \\ & + f_8(response_{t,d}) + f_9(mobility_{t,d}) + f_{10}(ORQ(density)_d) \\ & + f_{11}(elderly_d) + \beta_1(region = highland_d) \\ & + \beta_2(region = interior_d) \end{aligned} \quad (2)$$

Where $t$ is the date, $d$ is the district, $\beta_i$ represents the parametric coefficients of each category of the natural region factor variable, $f_i$ represents spline smooth functions of the continuous variables, and $ORQ(\ldots)$ signifies ORQ-transformed variables. A within-unit autoregressive correlation structure was specified to account for temporal dependence of observations in the same district. The modeled, adjusted associations were visualized in partial dependence plots of $R_t$ predictions across the range of values for each continuous exposure. Variable importance was assessed and ranked by computing the mean absolute accumulated local effects (ALE) of each predictor. To assess and compare relative effects, highly ALE-ranked variables were dichotomized at specific thresholds and otherwise identical GAMs refitted to calculate the percent differences in $R_t$ on unit-days above compared with below those thresholds (Colston et al., 2022). To quantify the variance explained by hydrometeorological relative to other variables, the $R^2$ of the final model was compared with that of an otherwise identical model that included only the non-hydrometeorological predictors. Data processing, visualization, and analysis were carried out using R 4.0.3 (R Core Team, 2020), Stata 16 (StataCorp, 2019), and ArcMap 10.8 (ESRI, 2019).

## Results

Data from the 3212 mainland districts of the three countries were included for the 245-day period from May 1 to December 31, 2020, resulting in a dataset with a total of 786 940 unit-day observations. Of these, 564 738 (71.8%) observations were excluded due to having both zero cases and an estimated $R_t$ value of between 0.95 and 1.05. A further 6952 (3.6%) of the remaining observations had missing mobility index data, leaving 184 870 complete observations to which the model was fitted.

Fig. 1 shows choropleth maps of the geographical distribution of cumulative COVID-19 cases and average SARS-CoV-2 $R_t$ (after applying exclusion criteria) summarized from daily values over the period of

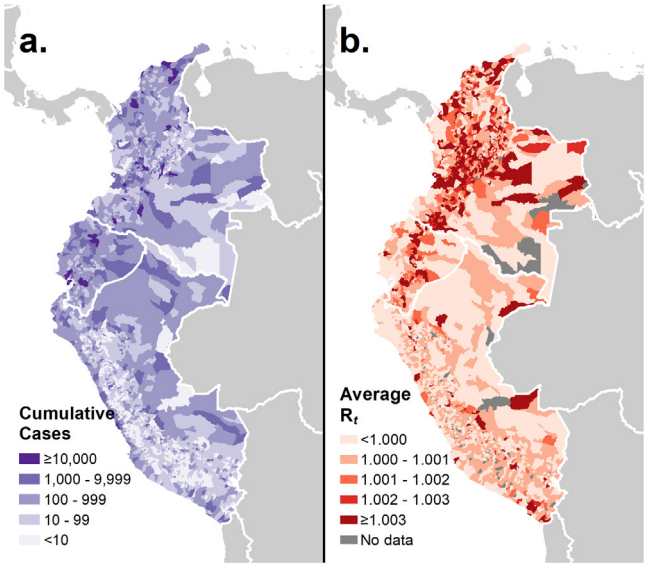


**Fig. 1.** District-level geographical distribution of cumulative reported COVID-19 cases and estimated SARS-CoV-2 reproduction number ($R_t$) in Colombia, Ecuador, and Peru (May 1–December 31, 2020)

analysis. Neither showed a marked geographical pattern, although cumulative case burden (Fig. 1a) exhibited notably lower values in the Peruvian highland districts, while many of the highest average $R_t$ values (Fig. 1b) were seen in the Ecuadorian and Colombian highlands. In Peru, the districts reporting more than 10 000 cases over the analysis period were in the Greater Lima Region as well as the other coastal cities of Trujillo and Chiclayo, while in Ecuador, aside from cantons of the three major cities of Guayaquil, Quito, and Cuenca, the much less populous canton of Cañar also exceeded this threshold. Colombia experienced more numerous pockets of high cumulative cases in the major metropolitan municipalities of its highlands — Bogotá, Medellín, Cali — and Caribbean coast — Barranquilla, Cartagena — as well as several relatively smaller cities, including Valledupar, Manizales, and Soledad.

Fig. 2 shows equivalent choropleth maps for averages of the six hydrometeorological variables. The lowest average temperature values (Fig. 2a) occurred along the Andes, particularly in the southern Peruvian stretch, while the highest occurred in the low-lying interior regions of the Amazon and Orinoco basins, as well as coastal Ecuador and Colombia. Relative humidity (Fig. 2b) and soil moisture (Fig. 2c) exhibited similar spatial distributions, with the highest average values in the interior areas of the three countries and along the Colombian coast, except for the arid Guajira peninsula, which had very low soil moisture content of $< 0.2$ $m^3/m^3$. Other areas of very low humidity and soil moisture included Peru's coastal Sechura Desert and Colombia's central Tatacoa Desert, as well as small pockets along the Ecuadorian coast. Average wind speeds (Fig. 2d) exceeded 1 m/s along most of the Pacific and Caribbean coasts, and in the high elevation Andean districts, while the mid-elevation windward and leeward Andean districts tended to have wind speeds of less than 0.5 m/s, as did parts of north central Colombia. Precipitation distribution (Fig. 2e) largely mirrored that of soil moisture and relative humidity, with the Guajira, Sechura, and Tatocoa Deserts experiencing low average daily rainfall of $< 1.5$ mm, and the Pacific coast and interior of Colombia exhibiting the wettest conditions. A belt of high solar radiation (Fig. 2f) extended along Peru's coast, which widened in the southeast to incorporate highland areas of the Andean plateau. The only other area with comparable radiation levels was on Colombia's Guajira peninsula.

Fig. 3 shows equivalent maps for the non-hydrometeorological covariates, including the extents of the three natural regions (Fig. 3d). The population of the three countries (Fig. 3f) is concentrated along the

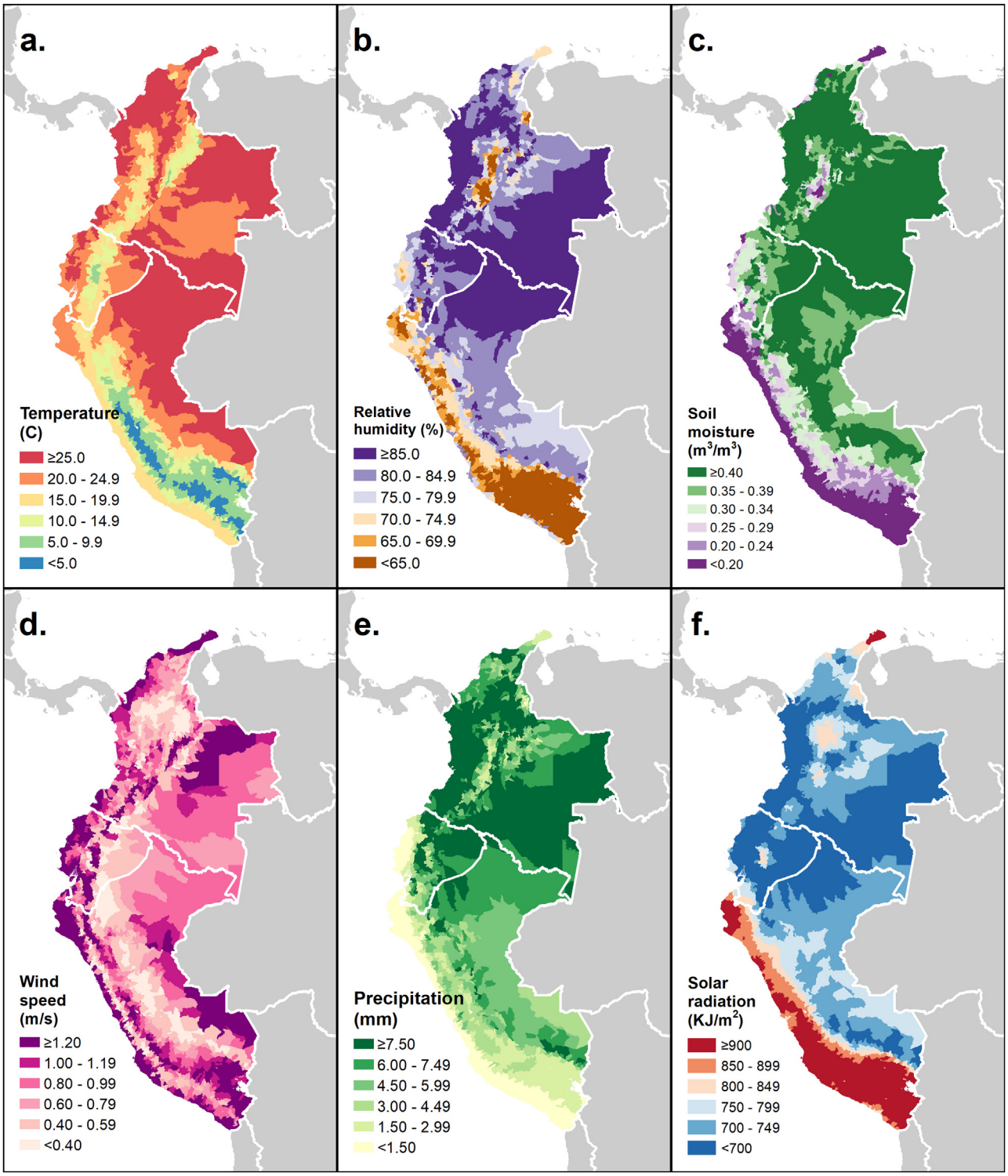


**Fig. 2.** District-level geographical distribution of six hydrometeorological variables in Colombia, Ecuador, and Peru (mean of daily averages, May 1–December 31, 2020)

coasts and highlands, with the exceptions of Colombia's sparsely populated Darién gap and the high elevation districts of Peru's southeast Andes. The population of the countries' interiors is not only sparse, but also most highly skewed towards the younger age groups (Fig. 3e), while the highlands and Peru's coastal plains have some of the districts with the highest percentage of population over 65 years. Access to healthcare, as measured by average travel time to the nearest health facility by motor transport (Fig. 3a), tends to vary inversely with population density, with the lowest levels of accessibility seen in the interior regions and along Colombia's Pacific coast, with the coasts and Andean highlands having the majority of districts with an average travel time of under an hour. Over the period from May to December, 2020, Peru had the most, and Ecuador the least, stringent policy response to the pandemic (Fig. 3b). Average time spent in residential locations (Fig. 3c) was highest (meaning mobility was lowest) in Peru's coastal and southern highland areas, in Ecuador's central highlands, and in the Capital

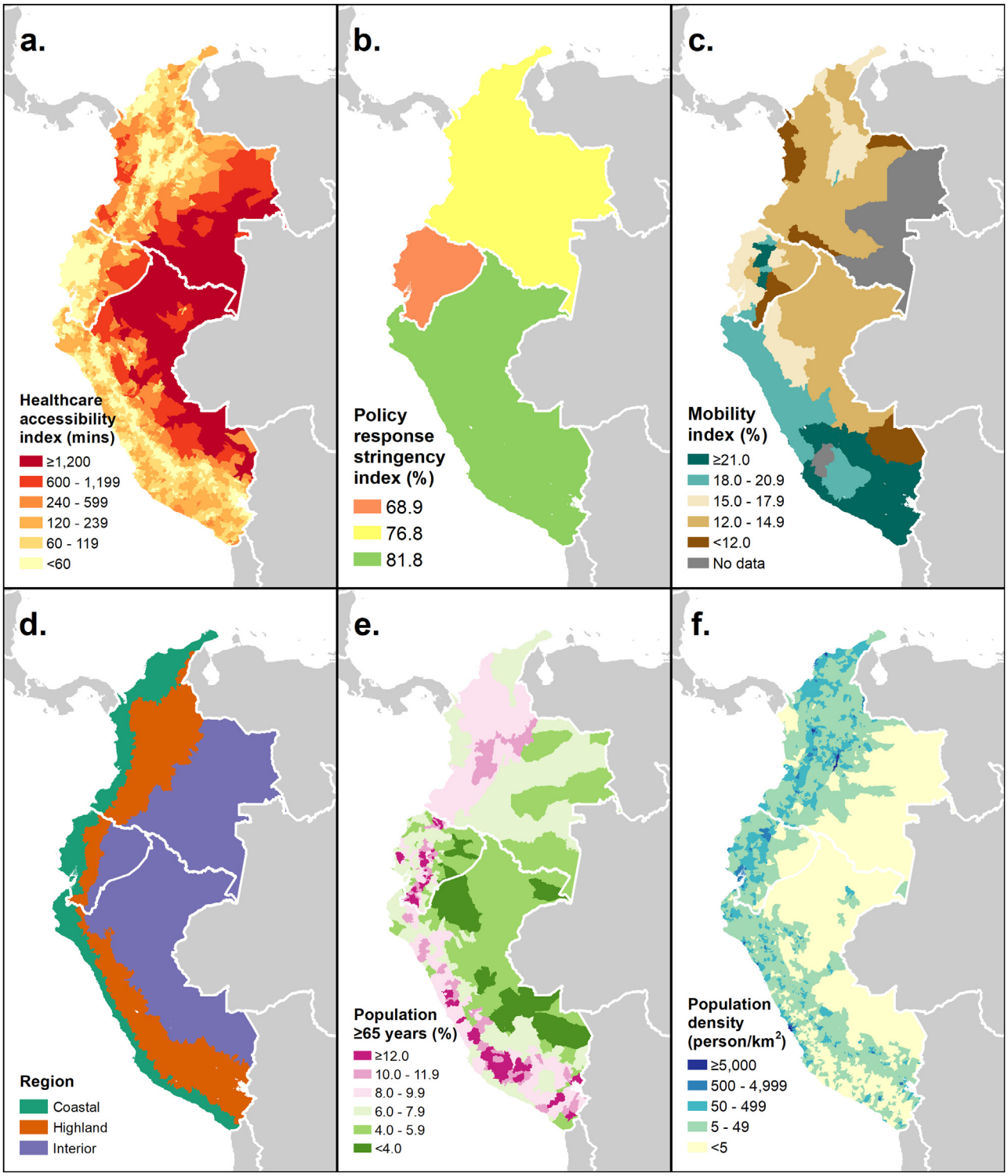


**Fig. 3.** District-level geographical distribution of six covariate variables in Colombia, Ecuador, and Peru (May 1–December 31, 2020)

District of Bogotá, Colombia, and lowest in provinces along the countries' land borders and Colombia's Pacific coast.

Fig. 4 shows the adjusted associations from the GAM. Precipitation and wind speed were ORQ-transformed due to their skewed distributions. Five of the six variables were highly statistically significantly associated with the outcome at the $\alpha < 0.0001$ level, the exception being wind speed, which was not significant at the $\alpha < 0.05$ level. The effect of temperature (Fig. 4a) on district-level $R_t$ was negligible in size, taking on a slight sinusoidal shape across the range of the variable's distribution. Precipitation (Fig. 4b) showed a broadly lop-sided U-shaped association with $R_t$, with the lowest predicted value in the mid-range and the highest at the upper extreme. The effect of soil moisture (Fig. 4c) was direct below a moisture value of approximately 0.35 $m^3/m^3$, before arcing back downward above that threshold. Solar radiation's association (Fig. 4d) took the form of a descending arc, with the inverse relationship most marked above a threshold of approximately 700 $kJ/m^2$, and the lowest

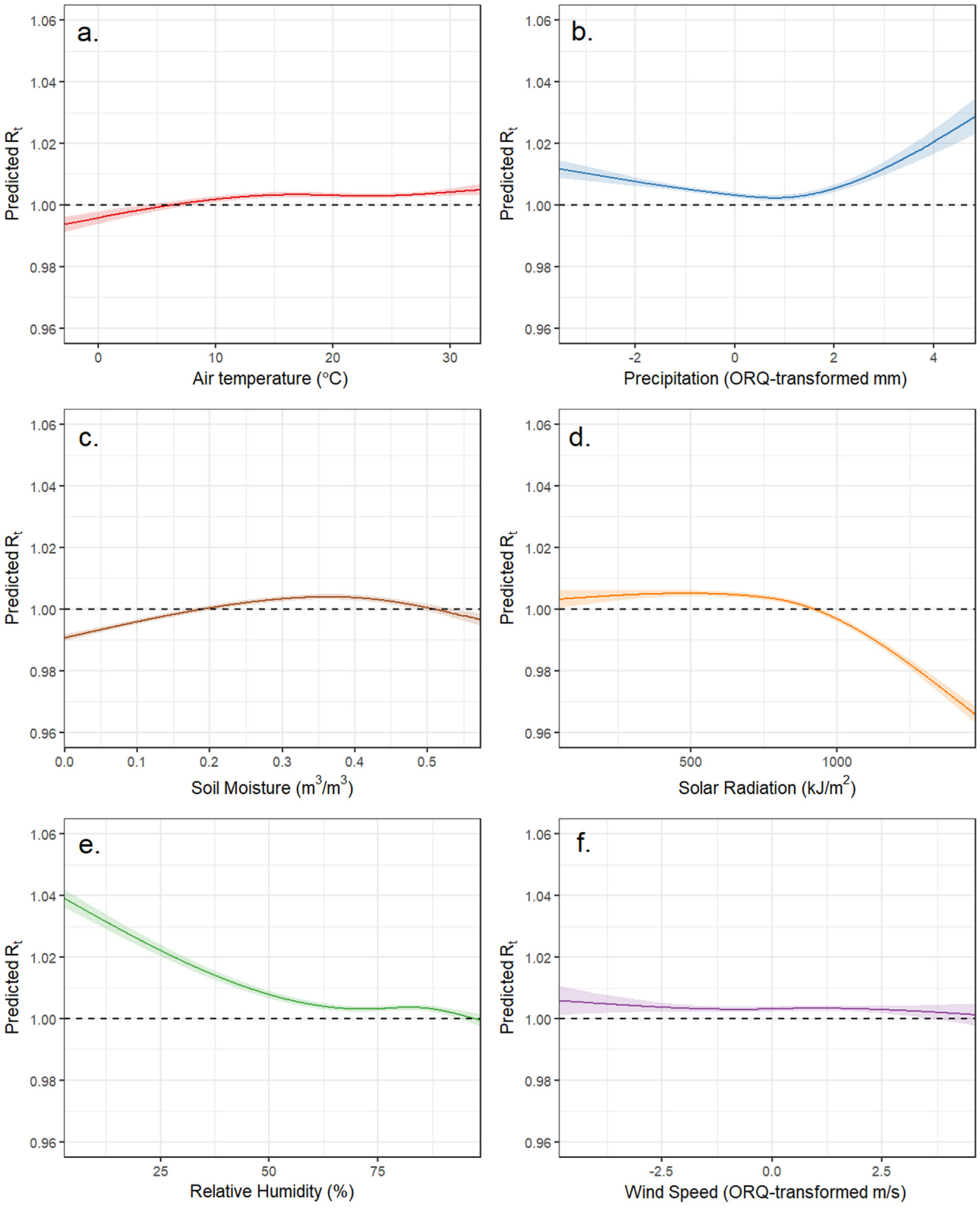


**Fig. 4.** Adjusted associations between six hydrometeorological variables and daily COVID-19 reproduction number ($R_t$ values) predicted by a generalized additive model

predicted $R_t$ for any of the hydrometeorological variables ($R_t < 0.97$) occurring at the upper radiation extreme of close to 1500 kJ/m$^2$. Relative humidity (Fig. 4e) had an effect size comparable to that of solar radiation, with increasing humidity mostly predicting decreasing $R_t$ (except for a plateau from around 70–80% relative humidity) and a difference in predicted $R_t$ of approximately 0.04 between the extremes of the distribution. No discernable association of wind speed with $R_t$ (Fig. 4f) was observed.

Fig. 5 shows the equivalent associations for the five continuous, non-hydrometeorological covariates and the coefficient estimates for the two

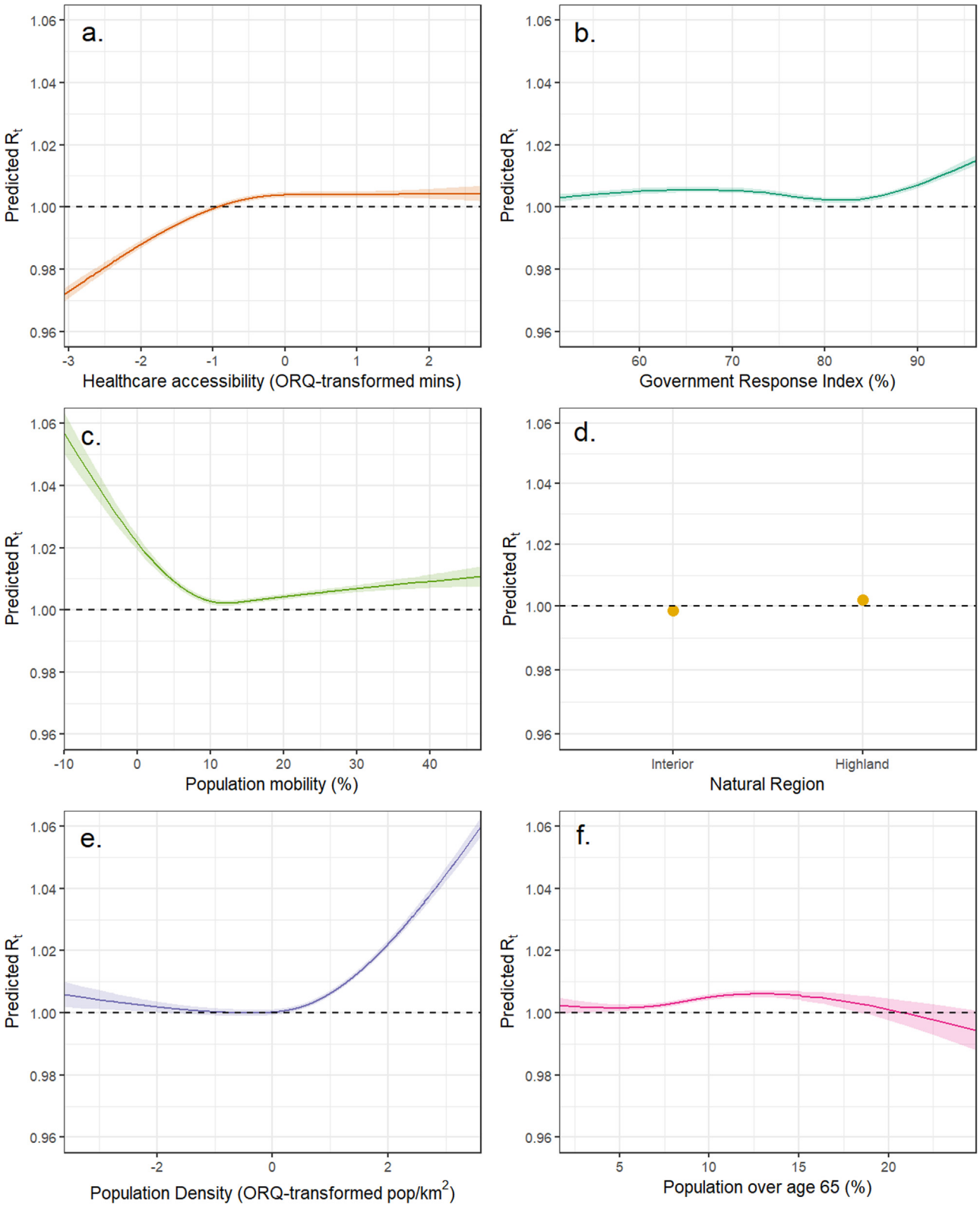


**Fig. 5.** Adjusted associations between six covariate variables and daily COVID-19 reproduction numbers ($R_t$ values) predicted by a generalized additive model

comparison natural region categories relative to the 'coastal' reference category. Population density and health facility accessibility were ORQ-transformed. $R_t$ increased with longer travel times to health facilities (Fig. 5a) from a value of 0.98 for the shortest time to just above 1 in the upper half of the ORQ-transformed accessibility distribution. The government response index (Fig. 5b) had a negligible effect on SARS-CoV-2 $R_t$ and did not predict a value below 1 at any value. Population mobility (Fig. 5c) had a large, steep inverse association with $R_t$ below a percent change of 10% — meaning that $R_t$ increased when time spent in residences showed little decrease or increased relative to the pre-pandemic

baseline — and a steady direct relationship above that threshold. The adjusted effects of the categorical natural region variable (Fig. 5d) were small yet statistically significant, particularly for the highland region. Population density (Fig. 5e) had a direct association with the outcome, with the most densely populated districts having an adjusted predicted $R_t$ of > 1.05, along with population mobility, with one of the largest effect sizes observed in this analysis. Though statistically significant at the $\alpha < 0.001$ level, the effect of population age structure (Fig. 5f) was negligible, consisting of a shallow, inverse U-shaped association, with a peak at roughly 13% of the population aged over 65 years.

The final model explained just 4.3% of the variance in the daily district SARS-CoV-2 $R_t$, compared with 2.8% by an equivalent model that excluded the hydrometeorological variables, and 2.3% by one that included only those variables. ALEs for all variables were correspondingly small (Supplementary Table S1), with population density ranking highest in terms of contribution to $R_t$ (ALE = 0.008), followed by healthcare accessibility (ALE = 0.005). In models in which the highest ALE-ranked variables were dichotomized (Table S1), differences in average predicted $R_t$ for unit-days on either side of variable-specific thresholds were also modest. Average adjusted $R_t$ was 0.9% lower on days in which relative humidity was higher than 50%, compared with less humid days, but 0.8% higher when soil moisture was above 0.1 $m^3/m^3$. Days in which solar radiation exceeded 1000 $kJ/m^2$ had 1.3% lower $R_t$, while the equivalent differences for districts in which average travel time to health facilities was more than half an hour and with a population density of more than 100 $pop/km^2$ were, respectively, increases of 0.4% and a 0.9%. On days in which mobility was reduced by 10% or more relative to pre-pandemic levels, $R_t$ fell by an average of 0.3%

## Discussion

The impacts of the COVID-19 pandemic on families, societies, and institutions have been incalculable. Furthermore, the notable spatiotemporal variability in these impacts is seemingly not fully attributable to population susceptibility and health system factors alone (Sorci et al., 2020), implicating a potential influence of climate and environment on the transmission and survivability of SARS-CoV-2 (Zaitchik et al., 2020). Early surveys of the evidence base highlighted a paucity of findings from the global South and tropical regions, insufficient spatiotemporal scope and resolution in analyses, and a failure to account for confounding from non-climatological factors (Kerr et al., 2021; Quintana et al., 2021; Smit et al., 2020; Zaitchik et al., 2020). More recently, as attempts to track the pandemic have coalesced into a wide variety of open datasets and online interfaces (Badr et al., 2021; Dong et al., 2020; Wahltinez et al., 2022), researchers have begun to address these knowledge gaps. Numerous recent studies have assessed effects on COVID-19 outcomes while adjusting for multiple hydrometeorological variables (Ma et al., 2020; Yuan et al., 2021) and other covariates, including population density (Smith et al., 2021), age structure (Landier et al., 2021), NPI compliance (Ganslmeier et al., 2021; Rubin et al., 2020), and government interventions (Ledebur et al., 2022), while others have focused on single countries in equatorial regions (Kerr et al., 2022; Lorenzo et al., 2021; Yin et al., 2022) or multiple countries and locations spanning wide latitudes and both hemispheres (Carleton et al., 2021; Sarkodie and Owusu, 2020; Sera et al., 2021). Our study is the first to bring together all these elements and at a high temporal resolution, with multiple, cross-cutting spatial scales, and for three neighboring countries that, despite including diverse populations and ecologies, share important commonalities in their pandemic experiences.

The ancestor of the SARS-CoV-2 index virus likely evolved through transmission among bats living in cool, dark, crowded caves (MacLean et al., 2021; Temmam et al., 2022). The primary direct, person-to-person mode of transmission of the pathogen is via virus-laden aerosols exhaled by infectious individuals, while an indirect route via contact with contaminated fomites is thought to make a minor contribution (Karia et al., 2020; Zhang et al., 2020). Small-scale atmospheric conditions, such as the temperature, pressure, and humidity of the air, affect the rates at which aerosolized respiratory droplets are formed, suspended, and dispersed, and thus influence disease transmission in complex ways (Ahlawat et al., 2020; Colston et al., 2019).

The negative association of relative humidity on SARS-CoV-2 $R_t$ identified here, among the largest absolute effect sizes of the hydrometeorological variables analyzed (though lower ranking by ALE), is consistent with one of the most widely documented of the disease's environmental sensitivities as well as current understanding regarding the virus's modes of transmission (Ahlawat et al., 2020; Hosseini, 2020). Whether quantified by absolute or relative measures, humidity has been shown to be an influential COVID-19 driver across many contexts (Majumder and Ray, 2021; Paraskevis et al., 2021), with very dry atmospheric conditions appearing to favor transmission, as has been shown for other respiratory (Lin and Marr, 2020) and non-respiratory (Colston et al., 2022) viruses. When expelled into dry air, respiratory microdroplets quickly shrink due to evaporation of their liquid content, allowing them to remain suspended for longer and increasing their viral particle concentration (Hosseini, 2020; Kumar and Morawska, 2019). Relative humidity also has a separate U-shaped association with SARS-CoV-2 viability outside the human host, with its lowest viability occurring at around 60% air saturation and its highest at the extremes (Ahlawat et al., 2020). Competing effects of decreasing transmissibility and increasing viability in the upper humidity extreme are consistent with the plateau effect seen in these results at relative humidities > 70%. In a contemporaneous study focused on Brazilian states in 2020 and 2021 (Kerr et al., 2022), humidity was also found to be the most important hydrometeorological variable; however, the direction of the humidity–$R_t$ relationship was opposite to the one found here.

Although there is less consensus surrounding the effect of temperature, it is widely supposed to have an association similar to that of humidity. Indeed, numerous studies have reported decreasing COVID-19 risk with increasing temperatures (Kerr et al., 2022; Landier et al., 2021; Paraskevis et al., 2021; Yuan et al., 2021). While this might at first glance seem to be at odds with the negligible and non-linear effect found in this analysis, comparisons with results specifically from other tropical settings suggest a more nuanced picture. One such study within a single season in Singapore (Lorenzo et al., 2021), in January to April, 2020, found a strong and significant direct association between temperature and COVID-19 case numbers, while another, also of a tropical, equatorial South American country (Brazil), found opposing effects of temperature in the March to May period (direct) compared with June to August (inverse) (Yin et al., 2022). Another study of > 400 cities across a wider range of latitudes in both the northern and southern hemispheres found a more complex, sinusoidally shaped relationship of temperature to transmission (Sera et al., 2021). Since the domain of this analysis spanned only tropical latitudes either side of the equator, the null-like finding for temperature could plausibly be the result of competing effects between the two hemispheres at different times over the year canceling each other out. However, marginal temperature effects predicted by multivariable models may be sensitive to the choice of humidity metric. The 400 city study adjusted for both relative humidity and absolute humidity (Sera et al., 2021), while a study of US counties that adjusted temperature for specific humidity found yet another complex and non-linear effect shape (Ma et al., 2021). This could reflect different drivers of transmission in temperate versus tropical climates. These three Andean countries generally have more tropical climates, with relatively small daily variations in hydrometeorological variables, whereas Brazil's climate spans tropical zones in its north and temperate zones in its south. Supplementary Figure S1 compares the results of this model with an otherwise identical one that substituted specific for relative humidity and reveals a somewhat more pronounced and direct effect of temperature in the specific humidity model. Temperature and specific humidity are closely related variables and exhibited multicollinearity in our dataset (a variance inflation for specific humidity of > 10 in models that included temperature). Moreover, certain combina-

tions of their values (e.g. low temperature with high specific humidity) simply do not occur naturally, so attempts to visualize effects of variations in one parameter while holding the other constant at its mean value are in some sense abstractions.

Our analysis also identified a sizeable, inverse association of solar radiation with COVID-19 transmission consistent with numerous other studies (Carleton et al., 2021; Majumder and Ray, 2021; Smith et al., 2021), most notably by Ma and colleagues, who also found this to be most pronounced above a threshold of ~1000 kJ/m$^2$ (Ma et al., 2021). Such findings have been interpreted as reflecting the deactivating effect of sunlight on SARS-CoV-2 virions, as has been observed in laboratory conditions in aerosols (Dabisch et al., 2021), on surfaces (Raiteux et al., 2021; Ratnesar-Shumate et al., 2020), and in mucus (Sloan et al., 2021). However, commentators have noted the difficulty of disentangling a direct effect of sunlight on the disease agent itself, from its confounding effect on host behaviors, such as rainy or cloudy weather driving people to congregate indoors, thereby increasing contact rates (Carleton et al., 2021; Colston et al., 2022). The fact that this effect was observed with adjustment for precipitation lends credibility to the supposed direct effect. Similarly, a substantial effect of precipitation was observed with adjustment for population mobility, the highest predicted $R_t$ occurring at the high end of the precipitation distribution, the lowest in the mid-range, and a secondary peak on rainless days. Given the absence of a waterborne route of transmission, it is tempting to attribute this to residual, unobserved confounding from host behaviors that are incompletely captured by the mobility variable, rather than a direct, causal impact of rainfall on virus dispersal. However, the role of aerosolized particles from wastewater cannot be ruled out (Senatore et al., 2021). In Andean countries like these, with wide inequities in sanitation coverage, many community-level environments are characterized by poor sewerage infrastructure (French et al., 2021), where open wastewater canals serve the dual functions of drainage for rainwater runoff, and conveyance of effluent discharge from household latrines (Berendes et al., 2019a). Such basic systems are easily overwhelmed by heavy rain events (Berendes et al., 2019b), which may promote the creation of airborne contaminated bioaerosols in which infectious pathogens can remain viable, as has recently been demonstrated for several enteropathogens, including viruses (Ginn et al., 2021).

Soil moisture was included as a negative control exposure, yet its observed effect on $R_t$, though small in absolute terms, was larger than that of government policy, population age structure, and natural region. A possible explanation is that soil moisture serves as a proxy for the general moisture retention of all surfaces, and that virus particles expelled in aerosolized droplets may remain viable for longer if they settle on a surface that permits them to retain their surrounding moisture (Colston, 2018). Wind speed was notable for being the only hydrometeorological variable with no association with $R_t$ among otherwise uniformly highly statistically significant effects. While there is little consensus in the published evidence regarding the effects of wind speed on COVID-19 transmission — several studies have reported inverse effects (Ganslmeier et al., 2021; Yuan et al., 2021), while others have reported direct (Ledebur et al., 2022; Majumder and Ray, 2021; Sarkodie and Owusu, 2020) or negligible associations (Yin et al., 2022) — this finding was unexpected. It seems otherwise highly plausible that faster wind speeds might suppress transmission of SARS-CoV-2 in outdoor environments by increasing air circulation and dispersing infective aerosols away from susceptible individuals, much as ventilation does in indoor environments (Clouston et al., 2021; Senatore et al., 2021). Indeed, in an otherwise identical unadjusted (single variable) model, a small, inverse effect of wind speed above a threshold high in the distribution was identified, consistent with that identified by Clouston and colleagues (Clouston et al., 2021) (Supplementary Figure S2).

The modeled effects of several non-hydrometeorological variables were consistent with the a priori hypotheses justifying their inclusion. Transmission was highest in densely populated districts, presumably due to higher contact rates, and lowest in districts with shorter travel time to health facilities, perhaps due to improved access to diagnosis and case management shortening the period between disease onset and isolation, or to unresolved confounding by latent urban status. On days in which time spent in residences was at least 10% more than was typical before the pandemic (a proxy for lockdown compliance), $R_t$ was statistically significantly reduced, though by less than 1% and not to a level below 1, which if sustained would eventually bring transmission under control. The proportion of the population that was elderly had no substantial impact on $R_t$, likely because old age is less of a risk factor for infectiousness or susceptibility to infection than it is for more severe COVID-19 outcomes once infected. It is striking that greater government response stringency had no effect on reducing $R_t$, and even appeared to increase it slightly in the upper extreme. This may reflect how government response is often slow and largely reactive to surges in cases, or that it has little impact over and above that which is mediated by individual behavior change and compliance — factors captured by the mobility variable.

This analysis was subject to certain limitations, in addition to those inherent to unit-level, ecological studies. The effect size estimates and proportions of variance in the outcomes explained by this model were smaller than those reported in other comparable analyses, in some cases by almost an order of magnitude (Sera et al., 2021; Ma et al., 2020). For example, in their analysis of the first wave of the pandemic in six North American and western European countries, Landier et al. found predicted $R_t$ values ranging from around 3.6 to 2.2 at the two extremes of the humidity distribution (Landier et al., 2021), while the equivalent range in Nottmeyer et al.'s multi-city analysis was around 1.55 to 0.8 (Nottmeyer et al., 2023), compared with the 1.04 to 1.0 found here. Ma et al. found 17.5% of $R_t$ variation in US counties to be attributable to three meteorological factors (Ma et al., 2021), compared with the 2.3% explained by six such factors in our analysis. There are several interrelated explanations for this. Firstly, we deliberately excluded from the time series the first wave of the pandemic during which transmission was highest and most unstable, which resulted in a narrower range of $R_t$ values, in line with evidence that the metric tends to center around a value of approximately 1 in most settings (Abbott et al., 2020). Secondly, the high level of geographical disaggregation meant that there was a large number of unit-days on which zero cases were reported or that had uninterpretable $R_t$ values. This also narrowed the distribution of outcome values, with an inflated number of observations close to 1, even after applying the exclusions (Supplementary Figure S3a and b). Given that environmental conditions vary on a very small scale and that case data were available at such high resolution, this was deemed a justifiable tradeoff. In a sensitivity analysis, the exclusion criteria were tightened such that unit-days with fewer than five cases (as opposed to zero) and an $R_t$ of between 0.95 and 1.05 were excluded. This further reduced the centralization of the distribution around the value of 1 (Supplementary Figure S3c), making it more Gaussian still, and led to effects of larger magnitude (Supplementary Figure S4 — note the change in $y$-axis scale) and an increase in explanatory power to 6.6%, when the model was refitted to the further restricted data and compared with the main results. This suggests that a lack of variability in the outcome partly explained the modest findings of this analysis. Lastly, limited variability in the exposures may also have played a role, since locations within this equatorial domain experience less changeable hydrometeorological conditions than other regions that have been examined. Supplementary Table S2 compares the average within-unit means and standard deviations of three such variables in the US county-level dataset used by Ma and colleagues (Ma et al., 2021) and the one used in our study over the same time period. While the average values were comparable, for all three variables, the location-specific variation (as measured by the within-unit standard deviation in the average) was considerably greater in the US dataset, which yielded larger effect sizes and weather-attributable $R_t$ variability (Ma et al., 2021).

In conclusion, COVID-19 transmission is sensitive to spatiotemporally varying hydrometeorological conditions in these three countries

of tropical Andean South America, even after adjusting for other potential confounders, including both static and time-varying variables, and at multiple cross-cutting scales. Dry atmospheric conditions of low humidity increased district-level SARS-CoV-2 reproduction numbers, while higher solar radiation decreased them. While several commentators have cautioned that the effects on transmission of climatological conditions are likely to be modest compared with factors such as NPI compliance (Carleton et al., 2021; Smit et al., 2020), these findings in fact show their influence to be of a comparable magnitude in several cases, and even greater than that of government response and population age structure. However, in absolute terms these effects, though significant, are modest and do not explain the excess disease burden experienced in some parts of this region during the first wave of the pandemic.

As SARS-CoV-2 settles into indefinite endemic circulation, it may be feasible to incorporate weather monitoring into disease surveillance and early warning systems alongside other more costly activities, such as wastewater or population seroprevalence surveillance, for anticipating case surges and allocating resources. Furthermore, population health interventions that encourage the public to exercise greater precautions on cloudy or dry days could also be considered. However, the high proportion of variance in COVID-19 transmission that remains unexplained, even after accounting for population factors and NPIs (> 96%), is striking, as are the negligible relative effect sizes of < 2%, which are far surpassed by those of interventions such as vaccination (53–94% — Andrews et al., 2022) and mask wearing (19% — Leech et al., 2022), all of which should serve as cause for caution when attempting to predict near-term changes in transmission risk.

## Author contributions

JMC, MNK, and BFZ conceived the study. MNK and BFZ secured funding for the research. JMC, PH, NHN, YTC, HB, and DNM carried out data processing, analysis, and visualization. MNK and AQ provided initial data. GHK, LMG, AQ, and FSS provided interpretation and writing support.

## Declaration of Competing Interest

All authors declare no conflicts of interest or competing financial interests.

## Acknowledgements

The authors are grateful to Ecuacovid, a project that provides a set of raw data extracted from reports on the national COVID-19 situation from Ecuadorian health authorities. https://github.com/andrab/ecuacovid.

## Data availability

The data and R code used in this analysis are provided as supplementary materials.

## Funding sources

The research presented in this article was supported financially by a COVID-19 supplement to NASA's Group on Earth Observations Work Programme (16-GEO16-0047), to Drs Zaitchik and Kosek. Additional funding was obtained from the Centers for Disease Control and Prevention (U01GH002270) to Dr Kosek. The funders played no role in the study design, the collection, analysis, and interpretation of data, the writing of the report, or the decision to submit the paper for publication. The findings and conclusions of this report are those of the authors and do not necessarily represent the official position of the funders.

## Ethical approval statement

There was no primary human or animal subject information used in the research, since the data were compiled entirely from publicly available secondary sources. Therefore, ethical approval was not sought. All data sources are properly attributed and cited.

## Supplementary materials

Supplementary material associated with this article can be found, in the online version, at doi:10.1016/j.ijregi.2022.11.007.

## References

Abbott S, Hellewell J, Thompson RN, Sherratt K, Gibbs HP, Bosse NI, et al. Estimating the time-varying reproduction number of SARS-CoV-2 using national and subnational case counts. Wellcome Open Research 2020;5:112. doi:10.12688/wellcomeopenres.16006.1.

Ahlawat A, Wiedensohler A, Mishra SK. An overview on the role of relative humidity in airborne transmission of SARS-CoV-2 in indoor environments. Aerosol Air Qual Res 2020;20:1856–61. doi:10.4209/aaqr.2020.06.0302.

Robalino Andrés N, Oporto Carlos, Hurtado Francisco. Serge Bibauw. Ecuacovid; 2021.

Andrews N, Tessier E, Stowe J, Gower C, Kirsebom F, Simmons R, et al. Duration of protection against mild and severe disease by Covid-19 vaccines. New England Journal of Medicine 2022;386:340–50. doi:10.1056/NEJMoa2115481.

Audi A, AlIbrahim M, Kaddoura M, Hijazi G, Yassine HM, Zaraket H. Seasonality of respiratory viral infections: will COVID-19 follow suit? Frontiers in Public Health 2020;8:576. doi:10.3389/fpubh.2020.567184.

Badr HS, Zaitchik BF, Kerr GH, Nguyen N-LH, Chen Y-T, Hinson P, et al. Unified real-time environmental-epidemiological data for multiscale modeling of the COVID-19 pandemic. MedRxiv 2021:2021.05.05.21256712. doi:10.1101/2021.05.05.21256712.

Barber RM, Sorensen RJD, Pigott DM, Bisignano C, Carter A, Amlag JO, et al. Estimating global, regional, and national daily and cumulative infections with SARS-CoV-2 through Nov 14, 2021: a statistical analysis. The Lancet 2022. doi:10.1016/S0140-6736(22)00484-6.

Berendes DM, Leon JS, Kirby AE, Clennon JA, Raj SJ, Yakubu H, et al. Associations between open drain flooding and pediatric enteric infections in the MAL-ED cohort in a low-income, urban neighborhood in Vellore, India. BMC Public Health 2019a;19:926. doi:10.1186/s12889-019-7268-1.

Berendes DM, de Mondesert L, Kirby AE, Yakubu H, Adomako Lady, Michiel J, et al. Variation in E. coli concentrations in open drains across neighborhoods in Accra, Ghana: the influence of onsite sanitation coverage and interconnectedness of urban environments. Int j Hyg Environ Health 2019b;224 –0.

Carleton T, Cornetet J, Huybers P, Meng KC, Proctor J. Global evidence for ultraviolet radiation decreasing COVID-19 growth rates. Proc Natl Acad Sci U S A 2021;118. doi:10.1073/pnas.2012370118.

Carlson CJ, Gomez ACR, Bansal S, Ryan SJ. Misconceptions about weather and seasonality must not misguide COVID-19 response. Nat Commun 2020;11:4312. doi:10.1038/s41467-020-18150-z.

Center for International Earth Science Information Network (CIESIN). Gridded Population of the World, Version 4 (GPWv4). Population Count; 2016.

Center for Systems Science and Engineering (CSSE) at Johns Hopkins University (JHU). COVID-19 Dashboard. Johns Hopkins University & Medicine Coronavirus Resource Center 2021 https://coronavirus.jhu.edu/map.html. (accessed October 12, 2021).

Chen S, Prettner K, Kuhn M, Geldsetzer P, Wang C, Bärnighausen T, et al. Climate and the spread of COVID-19. Sci Rep 2021;11:9042. doi:10.1038/s41598-021-87692-z.

Clouston SAP, Morozova O, Meliker JR. A wind speed threshold for increased outdoor transmission of coronavirus: an ecological study. BMC Infectious Diseases 2021;21:1194. doi:10.1186/s12879-021-06796-z.

Colston JM. Seasonality and hydrometeorological predictors of rotavirus infection in an eight-site birth cohort study: implications for modeling and predicting pathogen-specific enteric disease burden. Johns Hopkins University; 2018.

Colston JM, Ahmed T, Mahopo C, Kang G, Kosek M, de Sousa Junior F, et al. Evaluating meteorological data from weather stations, and from satellites and global models for a multi-site epidemiological study. Environ Res 2018;165:91–109. doi:10.1016/j.envres.2018.02.027.

Colston JM, Zaitchik B, Kang G, Peñataro Yori P, Ahmed T, Lima A, et al. Use of earth observation-derived hydrometeorological variables to model and predict rotavirus infection (MAL-ED): a multisite cohort study. Lancet Planet Health 2019;3:e248–58. doi:10.1016/S2542-5196(19)30084-1.

Colston JM, Zaitchik BF, Badr HS, Burnett E, Ali SA, Rayamajhi A, et al. Associations between eight earth observation-derived climate variables and enteropathogen infection: an independent participant data meta-analysis of surveillance studies with broad spectrum nucleic acid diagnostics. Geohealth 2022;6. doi:10.1029/2021GH000452.

Dabisch P, Schuit M, Herzog A, Beck K, Wood S, Krause M, et al. The influence of temperature, humidity, and simulated sunlight on the infectivity of SARS-CoV-2 in aerosols. Aerosol Science and Technology 2021;55:142–53. doi:10.1080/02786826.2020.1829536.

Dong E, Du H, Gardner L. An interactive web-based dashboard to track COVID-19 in real time. The Lancet Infectious Diseases 2020;20:533–4. doi:10.1016/S1473-3099(20)30120-1.

ESRI. ArcGIS Desktop: Release 10.8 2019.

Fernandes JSC, da Silva RS, Silva AC, Villela DC, Mendonça VA, Lacerda ACR. Altitude conditions seem to determine the evolution of COVID-19 in Brazil. Sci Rep 2021;11:4402. doi:10.1038/s41598-021-83971-x.
French MA, Fiona Barker S, Taruc RR, Ansariadi A, Duffy GA, Saifuddaolah M, et al. A planetary health model for reducing exposure to faecal contamination in urban informal settlements: baseline findings from Makassar. Indonesia. Environment International 2021;155. doi:10.1016/j.envint.2021.106679.
Ganslmeier M, Furceri D, Ostry JD. The impact of weather on COVID-19 pandemic. Sci Rep 2021;11:22027. doi:10.1038/s41598-021-01189-3.
Ginn O, Rocha-Melogno L, Bivins A, Lowry S, Cardelino M, Nichols D, et al. Detection and quantification of enteric pathogens in aerosols near open wastewater canals in cities with poor sanitation. Environ Sci Technol 2021. doi:10.1021/acs.est.1c05060.
Google LLC. Google COVID-19 Community Mobility Reports. 2022.
Hale T, Angrist N, Goldszmidt R, Kira B, Petherick A, Phillips T, et al. A global panel database of pandemic policies (Oxford COVID-19 Government Response Tracker). Nature Human Behaviour 2021;5:529–38. doi:10.1038/s41562-021-01079-8.
Haug N, Geyrhofer L, Londei A, Dervic E, Desvars-Larrive A, Loreto V, et al. Ranking the effectiveness of worldwide COVID-19 government interventions. Nature Human Behaviour 2020;4:1303–12. doi:10.1038/s41562-020-01009-0.
Hersbach H, Bell B, Berrisford P, Hirahara S, Horányi A, Muñoz-Sabater J, et al. The ERA5 global reanalysis. Quarterly Journal of the Royal Meteorological Society 2020;146:1999–2049. doi:10.1002/qj.3803.
Hosseini V. SARS-CoV-2 virulence: interplay of floating virus-laden particles, climate, and humans. Advanced Biosystems 2020;4. doi:10.1002/adbi.202000105.
Instituto Nacional de Estadística e Informática (INEI) and ICF International. Perú Encuesta Demográfica y de Salud Familiar - ENDES 2012. Lima, April 1, 2013.
Instituto Geografico Agustin Codazzi. Natural regions of Colombia. Geoportal 2014 http://geoportal.igac.gov.co/mapas_de_colombia/IGAC/Tematicos2012/RegionesGeograficas.pdf. (accessed October 12, 2021).
Instituto Nacional de Salud Colombiano. Casos positivos de COVID-19 en Colombia. Datos Abiertos Colombia 2021. https://www.datos.gov.co/en/Salud-y-Protecci-n-Social/Casos-positivos-de-COVID-19-en-Colombia/gt2j-8ykr (accessed October 12, 2021)
Karia R, Gupta I, Khandait H, Ashima Yadav, Anmol Yadav. COVID-19 and its modes of transmission. SN Comprehensive Clinical Medicine 2020;2:1798–801. doi:10.1007/s42399-020-00498-4.
Kerr GH, Badr HS, Barbieri A, Colston JM, Gardner LM, Kosek MN, et al. Evolving drivers of Brazilian SARS-CoV-2 transmission: a spatiotemporally disaggregated time series analysis of meteorology, policy, and human mobility, 2022. doi:10.1002/essoar.10512574.1.
Kerr GH, Badr HS, Gardner LM, Perez-Saez J, Zaitchik BF. Associations between meteorology and COVID-19 in early studies: inconsistencies, uncertainties, and recommendations. One Health 2021;12. doi:10.1016/j.onehlt.2021.100225.
Kumar P, Morawska L. Could fighting airborne transmission be the next line of defence against COVID-19 spread? City and Environment Interactions 2019;4. doi:10.1016/j.cacint.2020.100033.
Landier J, Paireau J, Rebaudet S, Legendre E, Lehot L, Fontanet A, et al. Cold and dry winter conditions are associated with greater SARS-CoV-2 transmission at regional level in western countries during the first epidemic wave. Sci Rep 2021;11:12756. doi:10.1038/s41598-021-91798-9.
Ledebur K, Kaleta M, Chen J, Lindner SD, Matzhold C, Weidle F, et al. Meteorological factors and non-pharmaceutical interventions explain local differences in the spread of SARS-CoV-2 in Austria. PLoS Comput Biol 2022;18. doi:10.1371/journal.pcbi.1009973.
Leech G, Rogers-Smith C, Monrad JT, Sandbrink JB, Snodin B, Zinkov R, et al. Mask wearing in community settings reduces SARS-CoV-2 transmission. Proceedings of the National Academy of Sciences 2022;119. doi:10.1073/pnas.2119266119.
Lin K, Marr LC. Humidity-dependent decay of viruses, but not bacteria, in aerosols and droplets follows disinfection kinetics. Environ Sci Technol 2020;54:1024–32. doi:10.1021/acs.est.9b04959.
Lorenzo JSL, Tam WWS, Seow WJ. Association between air quality, meteorological factors and COVID-19 infection case numbers. Environmental Research 2021;197. doi:10.1016/j.envres.2021.111024.
Ma Y, Pei S, Shaman J, Dubrow R, Chen K. Role of air temperature and humidity in the transmission of SARS-CoV-2 in the United States. MedRxiv: The Preprint Server for Health Sciences 2020. doi:10.1101/2020.11.13.20231472.
Ma Y, Pei S, Shaman J, Dubrow R, Chen K. Role of meteorological factors in the transmission of SARS-CoV-2 in the United States. Nat Commun 2021;12:3602. doi:10.1038/s41467-021-23866-7.
MacLean OA, Lytras S, Weaver S, Singer JB, Boni MF, Lemey P, et al. Natural selection in the evolution of SARS-CoV-2 in bats created a generalist virus and highly capable human pathogen. PLOS Biology 2021;19. doi:10.1371/journal.pbio.3001115.
Majumder P, Ray PP. A systematic review and meta-analysis on correlation of weather with COVID-19. Sci Rep 2021;11:10746. doi:10.1038/s41598-021-90300-9.
Mecenas P, Bastos RT da RM, Vallinoto ACR, Normando D. Effects of temperature and humidity on the spread of COVID-19: a systematic review. PLOS ONE 2020;15. doi:10.1371/journal.pone.0238339.
Meyer A, Sadler R, Faverjon C, Cameron AR, Bannister-Tyrrell M. Evidence that higher temperatures are associated with a marginally lower incidence of COVID-19 cases. Front Public Health 2020;8:367. doi:10.3389/fpubh.2020.00367.
Ministerio de Salud Peruano. Plataforma Nacional de Datos Abiertos. Plataforma Nacional de Datos Abiertos 2021. https://www.datosabiertos.gob.pe/dataset/casos-positivos-por-covid-19-ministerio-de-salud-minsa/resource/690e57a6-a465-47d8-86fd (accessed October 12, 2021)
Morales-Vives F, Dueñas J-M, Ferrando PJ, Vigil-Colet A, Varea MD. COmpliance with pandemic COmmands Scale (COCOS): the relationship between compliance with COVID-19 measures and sociodemographic and attitudinal variables. PLOS ONE 2022;17. doi:10.1371/journal.pone.0262698.
Morris DH, Yinda KC, Gamble A, Rossine FW, Huang Q, Bushmaker T, et al. Mechanistic theory predicts the effects of temperature and humidity on inactivation of SARS-CoV-2 and other enveloped viruses. ELife 2021;10:e65902. doi:10.7554/eLife.65902.
Mueller AL, McNamara MS, Sinclair DA. Why does COVID-19 disproportionately affect older people? Aging (Albany NY) 2020;12:9959–81. doi:10.18632/aging.103344.
Nottmeyer L, Armstrong B, Lowe R, Abbott S, Meakin S, O'Reilly KM, et al. The association of COVID-19 incidence with temperature, humidity, and UV radiation — a global multi-city analysis. Science of The Total Environment 2023;854. doi:10.1016/j.scitotenv.2022.158636.
Onyeaka H, Anumudu CK, Al-Sharify ZT, Egele-Godswill E, Mbaegbu P. COVID-19 pandemic: a review of the global lockdown and its far-reaching effects. Science Progress 2021;104. doi:10.1177/00368504211019854.
O'Reilly KM, Auzenbergs M, Jafari Y, Liu Y, Flasche S, Lowe R. Effective transmission across the globe: the role of climate in COVID-19 mitigation strategies. The Lancet Planetary Health 2020;4:e172. doi:10.1016/S2542-5196(20)30106-6.
Paraskevis D, Kostaki EG, Alygizakis N, Thomaidis NS, Cartalis C, Tsiodras S, et al. A review of the impact of weather and climate variables to COVID-19: in the absence of public health measures high temperatures cannot probably mitigate outbreaks. Sci Total Environ 2021;768. doi:10.1016/j.scitotenv.2020.144578.
Quintana AV, Clemons M, Hoevemeyer K, Liu A, Balbus J. A descriptive analysis of the scientific literature on meteorological and air quality factors and COVID-19. GeoHealth 2021;5. doi:10.1029/2020GH000367.
R Core Team. R: a language and environment for statistical computing. 2020.
Raiteux J, Eschlimann M, Marangon A, Rogée S, Dadvisard M, Taysse L, et al. Inactivation of SARS-CoV-2 by simulated sunlight on contaminated surfaces. Microbiol Spectr 2021;9. doi:10.1128/Spectrum.00333-21.
Ratnesar-Shumate S, Williams G, Green B, Krause M, Holland B, Wood S, et al. Simulated sunlight rapidly inactivates SARS-CoV-2 on surfaces. The Journal of Infectious Diseases 2020;222:214–22. doi:10.1093/infdis/jiaa274.
Rice BL, Annapragada A, Baker RE, Bruijning M, Dotse-Gborgbortsi W, Mensah K, et al. Variation in SARS-CoV-2 outbreaks across sub-Saharan Africa. Nature Medicine 2021;27:447–53 2021 27:3. doi:10.1038/s41591-021-01234-8.
Rubin D, Huang J, Fisher BT, Gasparrini A, Tam V, Song L, et al. Association of social distancing, population density, and temperature with the instantaneous reproduction number of SARS-CoV-2 in counties across the United States. JAMA Netw Open 2020;3. doi:10.1001/jamanetworkopen.2020.16099.
Sajadi MM, Habibzadeh P, Vintzileos A, Shokouhi S, Miralles-Wilhelm F, Amoroso A. Temperature and latitude analysis to predict potential spread and seasonality for COVID-19. SSRN Electronic Journal 2020. doi:10.2139/ssrn.3550308.
Sanderson E, Macdonald-Wallis C, Davey Smith G. Negative control exposure studies in the presence of measurement error: implications for attempted effect estimate calibration. Int J Epidemiol 2018;47:587–96. doi:10.1093/ije/dyx213.
Sarkodie SA, Owusu PA. Impact of meteorological factors on COVID-19 pandemic: evidence from top 20 countries with confirmed cases. Environmental Research 2020;191. doi:10.1016/j.envres.2020.110101.
Senatore V, Zarra T, Buonerba A, Choo K-H, Hasan SW, Korshin G, et al. Indoor versus outdoor transmission of SARS-COV-2: environmental factors in virus spread and underestimated sources of risk. EuroMediterr J Environ Integr 2021;6:30. doi:10.1007/s41207-021-00243-w.
Sera F, Armstrong B, Abbott S, Meakin S, O'Reilly K, von Borries R, et al. A cross-sectional analysis of meteorological factors and SARS-CoV-2 transmission in 409 cities across 26 countries. Nat Commun 2021;12:5968. doi:10.1038/s41467-021-25914-8.
Shenoy A, Sharma B, Xu G, Kapoor R, Rho HA, Sangha K. God is in the rain: the impact of rainfall-induced early social distancing on COVID-19 outbreaks. J Health Econ 2022;81. doi:10.1016/j.jhealeco.2021.102575.
Sloan A, Cutts T, Griffin BD, Kasloff S, Schiffman Z, Chan M, et al. Simulated sunlight decreases the viability of SARS-CoV-2 in mucus. PLOS ONE 2021;16. doi:10.1371/journal.pone.0253068.
Smit AJ, Fitchett JM, Engelbrecht FA, Scholes RJ, Dzhivhuho G, Sweijd NA. Winter is coming: a southern hemisphere perspective of the environmental drivers of SARS-CoV-2 and the potential seasonality of COVID-19. Int J Environ Res Public Health 2020;17:E5634. doi:10.3390/ijerph17165634.
Smith TP, Flaxman S, Gallinat AS, Kinosian SP, Stemkovski M, Unwin HJT, et al. Temperature and population density influence SARS-CoV-2 transmission in the absence of nonpharmaceutical interventions. Proceedings of the National Academy of Sciences 2021;118. doi:10.1073/PNAS.2019284118.
Sorci G, Faivre B, Morand S. Explaining among-country variation in COVID-19 case fatality rate. Sci Rep 2020;10:18909. doi:10.1038/s41598-020-75848-2.
StataCorp. Stata Statistical Software: Release 16, 2019.
Tarek M, Brissette FP, Arsenault R. Evaluation of the ERA5 reanalysis as a potential reference dataset for hydrological modelling over. North America. Hydrology and Earth System Sciences 2020;24:2527–44. doi:10.5194/hess-24-2527-2020.
Tatem AJ. WorldPop, open data for spatial demography. Scientific Data 2017;4. doi:10.1038/sdata.2017.4.
Telenti A, Arvin A, Corey L, Corti D, Diamond MS, García-Sastre A, et al. After the pandemic: perspectives on the future trajectory of COVID-19. Nature 2021;596:495–504. doi:10.1038/s41586-021-03792-w.
Temmam S, Vongphayloth K, Baquero E, Munier S, Bonomi M, Regnault B, et al. Bat coronaviruses related to SARS-CoV-2 and infectious for human cells. Nature 2022;604:330–6. doi:10.1038/s41586-022-04532-4.
Lancet The. COVID-19 in Latin America: a humanitarian crisis. The Lancet 2020;396:1463. doi:10.1016/S0140-6736(20)32328-X.

This is Ecuador. Ecuador y sus 4 regiones: Descubre su geografía. This isEcuador — the most complete guide to Ecuador 2021. https://www.thisisecuador.com/blog/ecuador-y-sus-4-regiones-descubre-su-geografia/(accessed October 12, 2021)

Uddin S, Imam T, Khushi M, Khan A, Ali M. How did socio-demographic status and personal attributes influence compliance to COVID-19 preventive behaviours during the early outbreak in Japan? Lessons for pandemic management. Pers Individ Dif 2021;175. doi:10.1016/j.paid.2021.110692.

Wahltinez O, Cheung A, Alcantara R, Cheung D, Daswani M, Erlinger A, et al. COVID-19 Open-Data: a global-scale spatially granular meta-dataset for coronavirus disease. Sci Data 2022;9:162. doi:10.1038/s41597-022-01263-z.

Wang C, Horby PW, Hayden FG, Gao GF. A novel coronavirus outbreak of global health concern. The Lancet 2020;395:470–3. doi:10.1016/S0140-6736(20)30185-9.

Wang H, Paulson KR, Pease SA, Watson S, Comfort H, Zheng P, et al. Estimating excess mortality due to the COVID-19 pandemic: a systematic analysis of COVID-19-related mortality, 2020–21. The Lancet 2022;0. doi:10.1016/S0140-6736(21)02796-3.

Weiss DJ, Nelson A, Vargas-Ruiz CA, Gligorić K, Bavadekar S, Gabrilovich E, et al. Global maps of travel time to healthcare facilities. Nature Medicine 2020;26:1835–8. doi:10.1038/s41591-020-1059-1.

Xia Y, Mitchell K, Ek M, Sheffield J, Cosgrove B, Wood EF, et al. Continental-scale water and energy flux analysis and validation for the North American Land Data Assimilation System project phase 2 (NLDAS-2): 1. Intercomparison and application of model products. Journal of Geophysical Research Atmospheres 2012;117:D03109. doi:10.1029/2011JD016048.

Yin C, Zhao W, Pereira P. Meteorological factors' effects on COVID-19 show seasonality and spatiality in Brazil. Environ Res 2022;208. doi:10.1016/j.envres.2022.112690.

Yuan J, Wu Y, Jing W, Liu J, Du M, Wang Y, et al. Association between meteorological factors and daily new cases of COVID-19 in 188 countries: a time series analysis. Sci Total Environ 2021;780. doi:10.1016/j.scitotenv.2021.146538.

Zaitchik BF, Sweijd N, Shumake-Guillemot J, Morse A, Gordon C, Marty A, et al. A framework for research linking weather, climate and COVID-19. Nat Commun 2020;11:5730. doi:10.1038/s41467-020-19546-7.

Zhang R, Li Y, Zhang AL, Wang Y, Molina MJ. Identifying airborne transmission as the dominant route for the spread of COVID-19. Proceedings of the National Academy of Sciences 2020;117:14857–63. doi:10.1073/pnas.2009637117.